

Behaviour of open-cell cordierite foams under compression

F.A. Costa Oliveira^{a,*}, S. Dias^a, M. Fátima Vaz^b, J. Cruz Fernandes^b

^a *Departamento de Materiais e Tecnologias de Produção (Edifício C), Instituto Nacional de Engenharia, Tecnologia e Inovação (INETI), Estrada do Paço do Lumiar, 22, 1649-038 Lisboa, Portugal*

^b *Department of Materials Engineering, The Technical University of Lisbon, Instituto Superior Técnico (IST) and Instituto de Ciência e Engenharia de Materiais e Superfícies (ICEMS), Av. Rovisco Pais, 1049-001 Lisboa, Portugal*

Received 30 June 2004; received in revised form 23 September 2004; accepted 1 October 2004

Available online 8 December 2004

Abstract

Cordierite foams were produced using the polymer foam replication method. The effects of both the structure of the polymeric foam template and the slurry's solid loads on the compressive strength and the sintered structure of the ceramic foam were evaluated in order to achieve the optimal manufacturing conditions. The compressive strengths of cordierite foams were measured at room temperature. Polyurethane (PU) foams were used as templates. Aqueous ceramic suspensions were prepared with solids weight fraction ranging from 50 to 65%. The effects of both the PU density and the solids volume fraction on porosity and strength of the developed cordierite foams were evaluated. The cordierite foams produced are of semiclosed-cell type. Some impregnation difficulties were experienced with increasing of the PU density. The compressive strength of the cordierite foams increased (from 0.1 to 2 MPa) with increasing solids volume fraction. These data are in agreement with the predictions of the model developed by Gibson and Ashby. However, the exponent of the model was half of the measured one (≈ 3) over the range of relative densities investigated (80–90%). Such discrepancy might be related to several factors such as the morphological differences in the structural unit of the developed foams with respect to a cubic open-cell foam or to the mixture of both open and closed cells or to the presence of non-periodic cells. In addition, it was found that the compressive strengths depended on the cell size for foams of similar relative densities and generally decreased with increasing of the cell size, which deviates from the theoretical predictions. When the starting polymeric substrate contained a higher fraction of closed cell windows, however, the ceramic material present on the cellular structure was not only distributed on the struts but also filled the cell walls. This contributed to an increase of the relative density of the cordierite foams and consequently to higher compressive strengths.

© 2004 Elsevier Ltd. All rights reserved.

Keywords: Replication process; Cellular ceramics; Mechanical properties; Cordierite; Substrates; Foams

1. Introduction

Open cell ceramic foams are being used mainly in applications where fluid transport through the microstructure is needed, including thermal insulation, molten metal filtration and hot gas cleanup, owing to their low bulk density, low thermal conductivity, low dielectric constant, very good thermochemical resistance and excellent thermal shock resistance.¹ In most applications damage produced by compressive loads

can lead to failure of these typically weak and fragile materials. The experimental data available on compression behaviour of brittle ceramic foams is extremely limited. Thus there is a need to understand failure mechanisms of these materials under compression loads in order to suggest ways of improving both macro and micro-structural designs. Cell size effect is often significant for brittle crushing with failure stresses usually increasing with decreasing cell size² and thus it should be taken into account in microstructural design.

There is also scarce information available in the scientific literature on the processing of ceramic foams. Several methods can be used to fabricate ceramic materials with a

* Corresponding author. Tel.: +351 210 924 600; fax: +351 217 166 568.
E-mail address: fernando.oliveira@ineti.pt (F.A.C. Oliveira).

cellular structure. The fabrication method chosen determines the range of porosity, the pore size distribution and the pore morphology. It is usually difficult to control void fraction and window size. Replication of polymeric foams offers a simple, inexpensive and versatile way of producing ceramic foams with pore sizes in the millimetre range but normally produces hollow struts. As the properties of ceramic foams are influenced by their structure³ relatively poor mechanical properties are achieved owing to processing-related flaws.^{4,5}

The choice of the ceramic material has been made on the basis of technical and commercial constraints. Cordierite has been selected owing to its low thermal expansion coefficient, adequate thermal conductivity and excellent resistance to thermal shock.⁶ As a low cost material, readily available and easily mass produced, it has proved satisfactory for automotive engine catalyst supports.

Although a number of theoretical models have been developed to describe the mechanical behaviour of cellular materials with respect to their relative density there is no experimental verification, to the author's knowledge, for the case of the compressive behaviour of cellular cordierite foams. Since most theoretical models can be satisfactorily applied only for relative density values (density ratio of the bulk density of the foam to the density of the cell struts and faces) lower than 0.2, processing parameters were set to allow ceramic foams to be obtained fulfilling this requirement. The motivation for the present study was therefore twofold: (a) to show the capability for microstructural control of cordierite ceramic foams by varying both the substrate polymeric materials and processing parameters as well as (b) to develop an understanding for the failure in compression of cordierite foams based on the relationship between the microstructure and the compressive behaviour. It was therefore the purpose of this study to identify ways of improving their mechanical properties as low compressive strength limits the loads that can be applied to these cellular ceramics.

2. Experimental procedure

Cordierite-based ceramic foams were fabricated by the replication method described elsewhere.⁷ Aqueous slurries with solid contents ranging from 50 to 65 wt.% were prepared from a powder mixture of materials (ball clays, talc, alumina and silica) that form cordierite upon firing (grade BL7 from Rauschert Portuguesa Ltd., Carcavelos, Portugal; specific surface area = $11 \text{ m}^2 \text{ g}^{-1}$ average particle size = $4.5 \mu\text{m}$ and true density = 2.91 g cm^{-3}). In order to ensure adequate rheological behaviour additions of 0.8 wt.% dispersant (Targon 1128, BK Ladenburg, F.R. Germany) and 2 wt.% binder (Sodium bentonite, MO34, Chemicer, Spain) were made based on the weight of dry solid added.

The open cell polyurethane (PU) foams used were four grades (hereafter referred to as 20DB, 22SB4, 28SBI and 25HR) of different densities (Table 1), which were manufactured by Flexipol – Espumas Sintéticas S.A., S. João

Table 1
Densities of the PU foams investigated

Foam grade	$\rho_{\text{PU}} \text{ (kg m}^{-3}\text{)}$
20 DB	21
22 SB4	22
25HR	25
28SBI	58

da Madeira, Portugal. Polyurethane foams were selected because they possess adequate resiliency, hydrophobic behaviour, ability to be uniformly covered and low temperature volatilisation without yielding noxious by-products making them suitable to produce fine (<1 mm cell size) ceramic foams.

Polyurethane foam samples (rectangular blocks of approximately $40 \text{ mm} \times 40 \text{ mm} \times 30 \text{ mm}$ before coating and firing) were dipped into the slurry and compressed to fill the void space. The excess slurry was removed by passing the samples through a set of rotating rollers at a fixed distance. After passing through the rollers the samples were placed on polished marble surfaces and allowed to dry at room temperature for at least 12 h. The samples were then placed in a drying oven featuring both temperature and humidity control. After drying the polyurethane foams were removed from the coated foam samples by a pyrolysis step in air using a slow heating rate ($1 \text{ }^\circ\text{C min}^{-1}$ to $500 \text{ }^\circ\text{C}$) and subsequently sintered at $1300 \text{ }^\circ\text{C}$ in an industrial gas furnace.

The bulk density and open porosity of the resultant foams were determined from the weight-to-volume ratio. The density of the solid struts was measured using an Accupyc 1330 pycnometer (Micromeritics, Norcross, GA, USA).

The foam morphology was characterised by scanning electron microscopy (SEM). Observations were carried out on a Philips XL 30 FEG scanning electron microscope using electron secondary beams at 1–2 kV. Several microstructural features of the polyurethane and cordierite foams have been determined using image analysis software and were discussed in more detail elsewhere.⁸ Based on the SEM images average values for the *cell equatorial diameter* L , the *struts thickness* expressed by its transverse length t , the *window shape* expressed by the 'aspect ratio', a.r., which is defined as the ratio between the major axis length and its perpendicular, and the *material volumic proportion*, V_v , were determined. The areas, perimeters and cell wall thickness were directly determined using a commercial image analysis software (Mocha).⁹ Cell lengths were obtained by the linear intercept method.¹⁰ For this purpose several parallel lines (equally spaced by 0.35 mm) were superposed on the micrographs and the number of cell walls intersected by unit length P_L was determined. The average cell length is then given by $L = 1/P_L$. A set of 120 measurements was carried out for each sample. The solid fraction of the foams V_v was determined through the ratio of the area occupied by the solid to the total area measured on each SEM micrographs. This implies that $1 - V_v$ is a measure of the foam porosity. The diameters were calculated assuming that cells have a circular section.

Table 2
Geometric density (ρ_{cf}), compressive strength (σ_{cf}) and porosity (ε) of the cordierite foams

Solid load (wt.%)		PU grade			
		20 DB	22 SB4	28 SBI	25 HR
50	ρ (g cm ⁻³)	0.29 ± 0.01	0.30 ± 0.01	0.28 ± 0.01	0.20 ± 0.01
	σ_{cf} (MPa)	0.24 ± 0.05	0.61 ± 0.04	0.47 ± 0.09	0.06 ± 0.01
	ε	0.89	0.89	0.89	0.92
55	ρ (g cm ⁻³)	0.30 ± 0.01	0.27 ± 0.01	0.27 ± 0.01	0.22 ± 0.02
	σ_{cf} (MPa)	0.34 ± 0.01	0.62 ± 0.05	0.70 ± 0.12	0.13 ± 0.03
	ε	0.89	0.90	0.90	0.92
60	ρ (g cm ⁻³)	0.35 ± 0.01	0.39 ± 0.02	0.35 ± 0.01	0.34 ± 0.05
	σ_{cf} (MPa)	0.84 ± 0.05	1.88 ± 0.08	Hollow	0.73 ± 0.07
	ε	0.87	0.85	0.87	0.87
65	ρ (g cm ⁻³)	0.51 ± 0.01	0.48 ± 0.02	0.42 ± 0.03	0.48 ± 0.02
	σ_{cf} (MPa)	1.59 ± 0.28	Hollow	Hollow	1.24 ± 0.14
	ε	0.81	0.82	0.84	0.82

Values are presented as the mean ± S.D. of the mean for four samples.



Fig. 1. Cross-section of 22SB4 cordierite foam impregnated in a slurry containing 65 wt.% solid load.

The compressive strength was measured according to the procedure described in a previous study¹¹ using a standard mechanical testing machine (Model 4302 Instron Corporation, Canton, MA, USA) fitted with a 10 kN load cell and flat steel plates closing with a cross head speed of 0.5 mm min⁻¹.

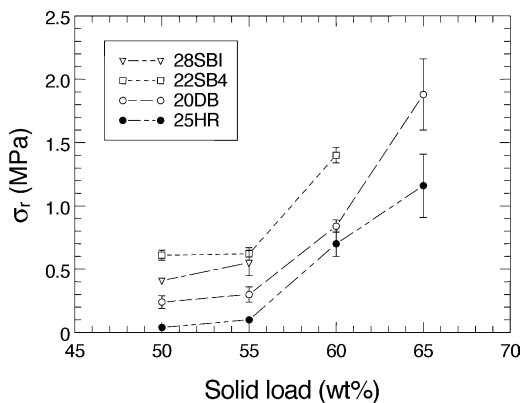


Fig. 2. Influence of slurries solid load on the compressive strength of the cordierite foams.

The cross-sectional area of the sample and the maximum failure load were used to calculate the fracture stress. As the surfaces of the foams were not entirely flat a compliant polymeric layer (2 mm thickness PVC) was used between the loading rams and the samples to assist in uniformly loading the bulk cordierite foams.

3. Results

The density of the cordierite foams fabricated by the replication method increased with increasing of the solid content in the slurries (Table 2). Some difficulties were experienced in impregnating the 28SBI type of foams. Under some conditions, cavities were observed in the core of the sintered foam samples. This is related to the higher density of this PU foam as compared to the others, which makes it difficult for the slurry to reach the interior of the foam. On the other hand, increasing the solids load above 60 wt.% has also resulted in difficulties in the impregnation of the 22SB4 type of foams in spite of its lower density. As illustrated in Fig. 1, cavities were also observed for samples made using 22SB4 polymer foams dipped into 65 wt.% solid load slurries. This suggests

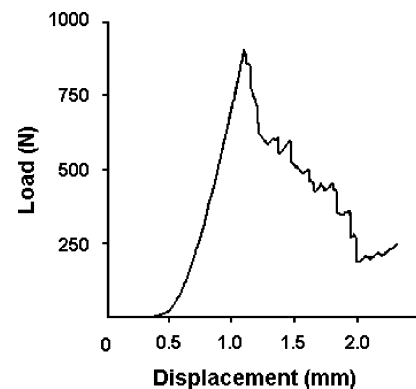


Fig. 3. Typical compressive test data for a cellular cordierite foam sample.

that ideally one should select polymeric foams of low density and open-cell structure since the presence of closed cell windows hinders the access of the slurry to the core of the polymeric substrate.

The compressive strength was found to increase with increasing of the solids volume fraction as expected (Fig. 2). Fig. 3 shows a typical load–displacement curve for the cordierite foams under compression testing. In the initial stage the load increased linearly. This corresponds to the lin-

ear elastic behaviour for the typical fracture of brittle foams. When the applied load exceeded a given value the sample started crushing and struts begun failing prior to attaining the maximum stress (presumably weaker struts or those aligned in a favourable direction for maximum stress). The compressive strength was determined from the point in the chart recorder where the load reached its maximum. At the crushing point propagation of macroscopic cracks has resulted in a load drop. Additional deformation of the foam occurs as

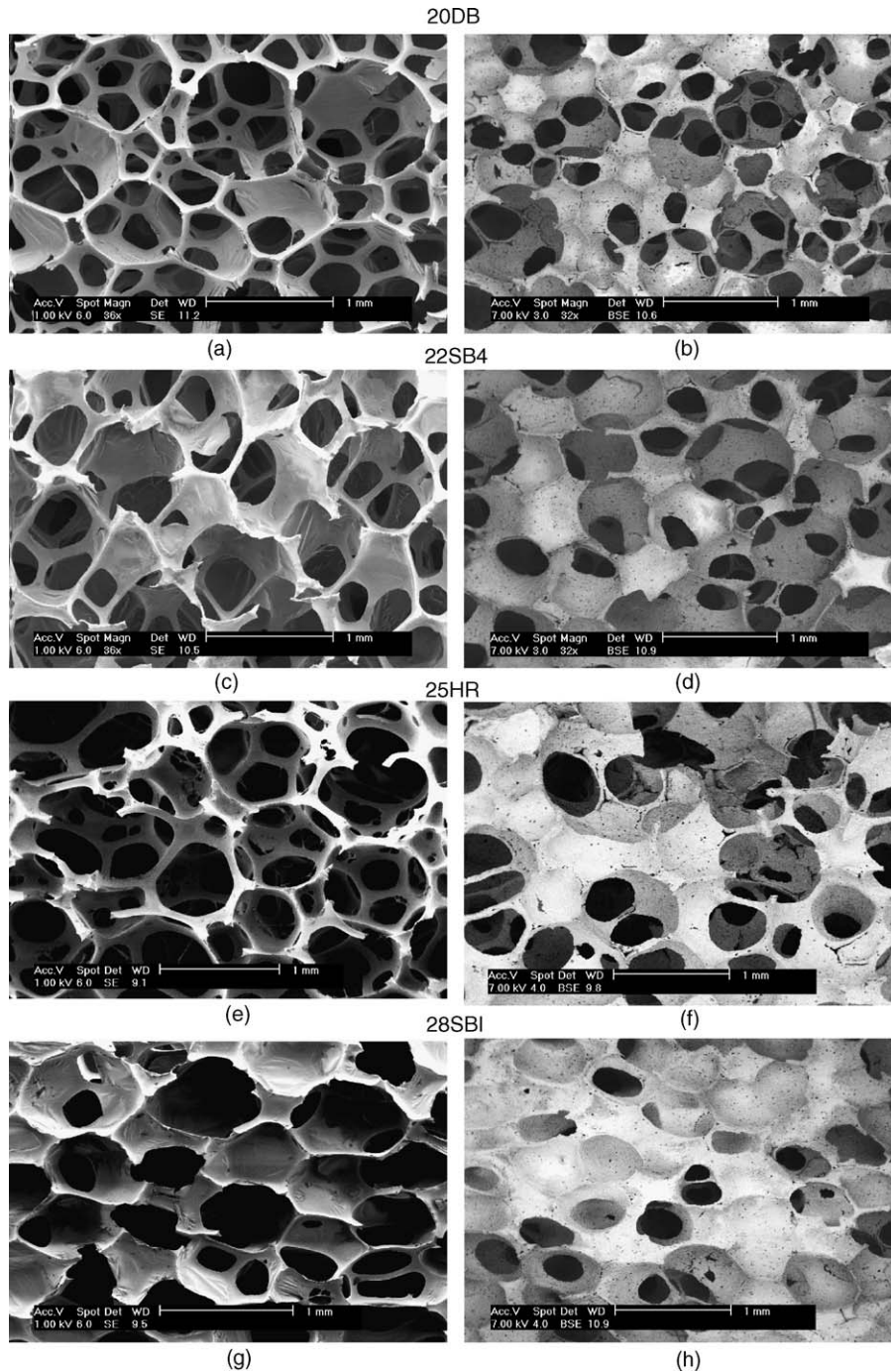


Fig. 4. Typical SEM micrographs showing the microstructure of polymeric foam templates (a, c, e, g) and the corresponding cordierite foams (b, d, f, h).

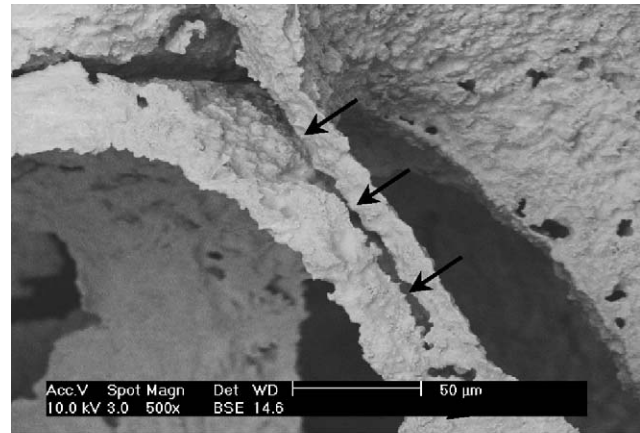
the sample becomes progressively damaged (layer by layer) from either the top or the bottom owing to breakage of struts. It was observed that struts were failing prior to attaining the maximum stress and that the failure of these struts was accompanied by slight drops in the load/displacement curve. As noticed the compressive strength was not associated with the failure of a single strut but rather with the propagation of either a macroscopic crack or multiple cracks after damage accumulation has reached a critical level.

Typical macrostructures of the sintered foams are shown in Fig. 4. These foams were found to consist of a three-dimensional array of struts. The cells shape of the cordierite foam is polyhedral and show preferential orientation associated with the polyurethane rise direction. Some of the cell windows are covered with a thin ceramic membrane. Longitudinal strut cracks were observed (Fig. 5a) at the relatively sharp edges of the hollow triangular cross-section struts of the PU substrate (Fig. 5b). The major processing problem arises from difficulties in coating the sharp edges with the slurries. After coating, the thickness of slurry in these areas is lower than elsewhere. It is apparent that the triangular cross-section of the polymeric foam struts originates strength limiting flaws in the ceramic foam. To overcome this problem, it would be useful to apply some process that could make the cross-section of the PU foams become less angular.

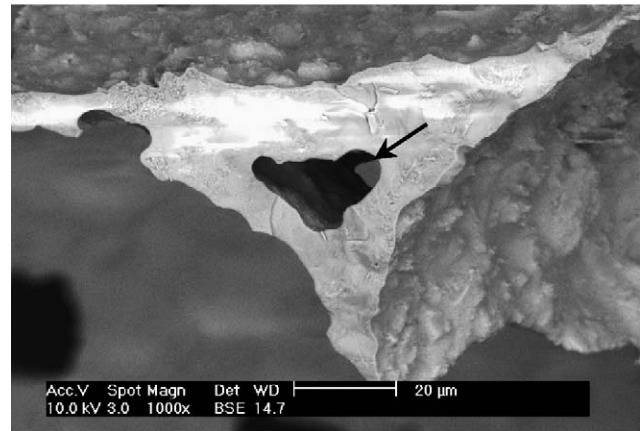
Table 3 lists the main macrostructural features measured on both polymeric and corresponding cordierite foams. As indicated by the aspect ratio of the cells are elongated in the rising direction of the PU foams. This means that the assumption, which has been made in the diameter determination, only provides a rough estimate of the true cell diameter.

4. Discussion

The use of 28SBI foam templates of high density ($>50 \text{ kg m}^{-3}$) and small cell size ($<600 \mu\text{m}$) has resulted in impregnation problems, particularly for slurries with solid loads above 55 wt.%, as anticipated. However, it is interesting to note that the compressive strength of cordierite foams made from such templates at 55 wt.% solid load showed higher compressive strengths (σ_{cf}) than all the others. This is most likely related to the structure of the resulting foams, as most



(a)



(b)

Fig. 5. SEM photographs of a sintered open cell cordierite sample showing (a) a longitudinal crack on the strut surface and (b) the hollow nature (triangular void) of the cell struts.

of the cells consisted of closed windows. The larger scatter in σ_{cf} data for this type of substrate is associated with the difficulties in distributing uniformly the slurry within the polymeric foam. In spite of its lower density, 22SB4 foams were also difficult to impregnate. Nonetheless, the highest σ_{cf} values were recorded when using this type of template for a solid load of 60 wt.%. Once again, this is attributed to the structure of the foam rather than the cell size. As shown in Fig. 4, PU foams of the 22SB4 grade consisted of cells with

Table 3
Microstructural characterisation of the PU substrates and the cordierite foams made from slurries containing 60 wt.% solids

Foam grade	Cell mean diameter, \bar{L} (μm)	Strut mean thickness, \bar{t} (μm)	Cell mean perimeter, \bar{P} (mm)	Solid volume fraction, V_v	Window shape, <i>a.r.</i>
POLYMER 20DB	715 ± 129	59 ± 16	2.53 ± 0.46	0.11 ± 0.04	1.38 ± 0.13
22SB4	888 ± 35	79 ± 22	3.28 ± 0.10	0.14 ± 0.01	1.07 ± 0.04
28SBI	589 ± 72	58 ± 15	2.15 ± 0.30	0.10 ± 0.01	1.42 ± 0.09
25HR	930 ± 119	77 ± 21	3.28 ± 0.52	0.11 ± 0.01	1.11 ± 0.25
CERAMIC 20DB	575 ± 55	59 ± 14	2.02 ± 0.22	0.13 ± 0.02	1.16 ± 0.05
22SB4	717 ± 21	58 ± 16	2.51 ± 0.14	0.16 ± 0.02	1.09 ± 0.02
28SBI	524 ± 78	71 ± 15	1.88 ± 0.28	0.19 ± 0.02	1.34 ± 0.08
25HR	716 ± 93	93 ± 26	2.50 ± 0.35	0.16 ± 0.01	1.21 ± 0.25

Values are presented as the mean ± S.D. of the mean of 120 cell measurements.

a higher content of closed thin windows than those of grades 20DB and 25HR. Since the cordierite foams replicated the polymeric ones, the contribution of these closed windows to the overall structure cannot be neglected.

The compressive strength of ceramic foams depends on various factors such as the structure and the relative density. Both the macrostructure (i.e. the arrangement of cells) and the microstructure (for instance, the presence of cracks within the struts), have a strong influence on the mechanical behaviour of the ceramic foam.

Studies of brittle cellular materials have demonstrated a relationship between the compressive strength (σ_{cf}) and relative density (ρ_{cf}/ρ_s). Assuming that the unit cell for open-cell materials is represented as a cubic array of struts of square cross section t and length L , Gibson and Ashby^{12,13} developed models capable to explain the mechanical behaviour of these materials providing that the deformation mode of the struts and walls is correctly identified. The bending micromechanical model developed by Gibson and Ashby (hereafter referred to as GA model) assumes that the mechanics of a unit cell can be applied to describe the overall deformation behaviour of the foams and that the dependence of σ_{cf} on ρ_{cf}/ρ_s of brittle foams relies on the fact that collapse occurs when the bending moment being applied to the struts reaches the fracture moment:

$$M_f = \frac{1}{6} \sigma_{fs} t^3 \quad (1)$$

where σ_{fs} is the fracture strength of the strut material (i.e. 65 ± 5 MPa for dense cordierite).⁶ Under these conditions the compressive strength of the foam σ_{cf} can be calculated through the relationship:

$$\frac{\sigma_{cf}}{\sigma_{fs}} = C_1 \left(\frac{\rho_{cf}}{\rho_s} \right)^{3/2} \quad (2)$$

where ρ_{cf} is the bulk density of the ceramic foam, ρ_s is the density of the solid struts (2.62 g cm^{-3} , measured by pycnometry) and C_1 is a geometric constant characteristic of the unit cell shape found to be equal to 0.65 for brittle open-cell foams by fitting the theoretical equation to limited data.¹⁴ Zhang and Ashby derived an analytical solution for this constant, assuming tetrakaidecahedral unit cell geometry, and suggested a value of 0.16.¹⁵ The experimental compressive strength data in Table 2 were plotted versus the relative density and evaluated using the GA model for brittle cellular foams. The compressive results deviated significantly from the model, as an exponent of ≈ 3 was obtained (i.e. twice as large as that predicted by Eq. (2)). This is not surprising in view of the fact that the GA model for compressive failure of brittle open-cell foams is based on the catastrophic collapse of cells at a critical stress value whereas we assume the cordierite foams to fail by a damage accumulation process. Other model limitations concern non-periodic and disordered cells, the proportion of open and closed cells and the microstructural defects, cracks within the struts.

The damage accumulation process was also observed by Brezny and Green.¹⁵ Plotting their experimental data for open cell alumina-mullite foams, we obtained an exponent of 2.2. On the other hand, Colombo et al.³ have also reported an exponent of 3.6 for silicon oxycarbide foams under compressive loads. The value of the exponent not only varies in accordance to the micromechanical model used but also depends on the proportion of open and closed cells and on the mechanism of load transfer among the various constituents of the structure.¹⁶ In view of the fact that the loading system used was rigid and the surfaces of the foams were not entirely flat, a compliant layer was used to correct misalignments thus allowing the load to be transferred in a more uniform fashion. The difficulties in uniformly loading these porous materials may also account for the discrepancy between the experimental data and the theoretical models. This issue has yet to be solved in spite of suggestions made for the use of compliant rams.¹⁷ In the case of the cordierite foams produced in this study, the exponent is higher than that predicted by the GA model for closed-cell foams (the exponent is 3/2 or 2, depending on the cell morphology being open or closed cell, respectively). This is not surprising since the morphology of the foams obtained by the replication method is more similar to a closed foam rather than to a reticulated (open-cell) one. In fact, cell windows are present in most cell walls, as shown in Fig. 4. This does not mean that the porosity is not interconnected and therefore they can still be considered as open cell foams.

For most porous solids, the relationship between cell (pore) size (L) and porosity (ε) is extremely complex. Indeed, it is difficult to isolate their influence on the mechanical properties of these materials. It is well accepted that the increase in mechanical strength through reduction in the porosity is associated with cell size decrease. Either increasing void volume (porosity) or cell size within the structure will, however, cause a decrease in the mechanical strength. Gibson and Ashby¹³ showed that for low density foams ($\rho_{cf}/\rho_s < 0.1$), with open cells, a relationship between ε and D is valid:

$$\frac{\rho_{cf}}{\rho_s} = 1 - \varepsilon = C \left(\frac{t}{L} \right)^2 \quad (3)$$

where t is the strut thickness and C is a geometric constant close to one. This equation is only valid if the ratio t/L remains constant as the pore size varies; in other words, only if t increases proportionally to the pore diameter. This only happens if processing permits porosity to remain constant for different pore sizes. Considering the slight variance of porosity in ceramic foams, Eq. (3) has a limited range of applicability. Nonetheless, the relationship between ceramic foam properties and porosity is still widely used:

$$\frac{\text{foam property}}{\text{solid property}} = C_i (1 - \varepsilon)^{n_i} \quad (4)$$

where C_i and n_i are constants depending on the foam structure. Dam et al.¹⁷ have proposed that:

$$\sigma_{cf} = C\sigma_{fs}A(1 - \varepsilon)^{2.2} \quad (5)$$

where A is a constant equal 0.30. As $\varepsilon = 1 - \rho_{cf}/\rho_s$, this equation is equivalent to Eq. (2) but with a higher exponent. An important feature of the cordierite foams made by the replication method that is not accounted for in the theoretical development is the hollow nature of the cell ceramic struts, due to volatilisation of the organic foam substrate (as seen in Fig. 5). It is straightforward to modify the equation proposed by Gibson and Ashby to account for this effect. Considering that the (square) struts in the micromechanical model of Gibson and Ashby contain a square hole of dimension t' , at low densities, one can rewrite Eq. (2) to

$$\sigma_{cf} \approx C\sigma_{fs} \left\{ \left(\frac{t}{L} \right)^2 \left[1 - \left(\frac{t'}{t} \right)^2 \right] \right\}^{1.5} \quad (6)$$

owing to the fact that $\rho_{cf}/\rho_s \approx (t/L)^2$. Hence, the hollow nature of the struts will reduce the moment of inertia of the cell struts by a factor of $[1 - (t'/t)^4]$.¹⁸ This is regarded as the main cause for the low mechanical strength that characterise this type of structure.

As shown in Fig. 5, the actual strut geometry consists of beams containing an internal triangular hole. Assuming that these beams are rigidly supported at both ends, under the action of a central point force, Brezny et al.¹⁹ derived the following equation to determine the strut strength (σ_{ft}) as

$$\sigma_{ft} = \frac{36PLD}{9\pi D^4 - 16bh^3} \quad (7)$$

where P is the fracture load, D is the outside diameter of the strut, and b and h are the base and height of the triangular hole within the strut. If the beam is not rigidly supported, the strength is actually higher than that predicted by Eq. (7). Additional errors are associated with the fact the compliance of the nodal supports can vary depending on the number of struts which are connected to it. The compliance can be further reduced by the presence of cracks formed during polymer burnout, as shown in Fig. 5.

To design a foam, one should also take into account size effects when developing these very porous materials. In fact, large samples fail at lower stresses than small ones simply because the probability that they contain a larger pre-existing flaw is higher. Brezny and Green⁴ showed that not only σ_{cf} decreased linearly with increasing cell size for reticulated vitreous carbon foams but also that failure was attributed to localised damage within a region ultimately resulting in collapse of a band of cells perpendicular to the direction of loading. For this type of foam a relatively narrower distribution of strut strengths (higher Weibull modulus, e.g. $m_W = 6$) was obtained. Instead for alumina-mullite foams possessing hollow struts with a large number of processing defects (and consequently a wider distribution of strut strengths, $m_W = 3$), they observed a gradual degradation of compressive strengths.

This could be associated with linking of pre-existing microcracks. Thus, it is likely that the cordierite foams under investigation failed in a similar manner to the alumina-mullite foams.

The compressive strengths for the foams investigated in the present work increase with the total volume fraction of ceramic as predicted by Eq. (2). If one considers Eq. (3), it is expected that t/L will increase with increasing density, but as seen in Table 3, this ratio does not change appreciably (0.08–0.14). Not surprisingly, the cordierite foams made from 22SB4 polymeric templates showed the lowest ratio, indicating that the material which is added to increase the density of the structure is not distributed uniformly on the struts but rather goes to fill closed cell windows. This clearly complicates the use of Eq. (2) for this type of cellular materials.

A consistent trend of higher σ_{cf} values was observed for cordierite foams derived from 20DB polymeric foam substrates as compared to 25HR foams in spite of their similar bulk densities. This is related to higher relative densities obtained for the 20DB type of foams. This contrasts with the expectation that materials with higher t/L would lead to higher relative densities (cf. Eq. (3)), thus indicating that the compressive strength is closely related to the structure of the cells network. In this particular case, the reduction of cell size can also play a role in the overall compression performance, as smaller cell sizes should increase compressive strength.

It appears from this work that the compression behaviour as a function of the relative density is rather difficult to model accurately. There seems to be a close relationship between σ_{cf} and the structure of the material (in particular the proportion of open and closed cell windows, the defect population and the cell geometry). Therefore, one needs to eliminate strut cracks and other large flaws in order to increase the strength of the individual struts during the fabrication process so that maximum strength in the bulk foam can be achieved.

5. Conclusions

This work has brought insight into the effect of some critical manufacturing parameters of ceramic foams by the replication method, namely the ceramic solid load in the slurries and the density, cell size and microstructural network geometry of polyurethane foam templates, on the compression behaviour of brittle open-cell cordierite foams. The use of different PU substrates allowed the fabrication of open-cell cordierite foams with a variable morphology, and therefore different properties. The compressive strength of the cordierite foams increased with increasing relative density in accordance to theoretical predictions. However, there seems to be some influence of the distribution of strut strengths on the compressive behaviour as these foams contain a large number of pre-existing cracks and defects resulting from the manufacturing process. Under compressive loading, these cellular materials failed by a damage accumulation process

rather than by catastrophic collapse of cells perpendicular to the direction of loading. It is postulated that the accumulation of damage occurs at two levels: within the struts and within the macrostructure. Hence, the compressive strength dependence on the structure of the ceramic foam is not easy to predict since the strength of the struts has a direct effect on that of the foam. It has also been shown that foams with larger cell sizes (cf. 22SB4 versus 20DB) do not necessarily possess lower resistance in compression. This suggests that further work should focus on the understanding of the relation between the material behaviour under compression and its structure so that new materials with improved performance can be developed. Although limited data is yet available to establish a sound relationship between compressive strength and cell dimensions, the results of the present work clearly suggest that the inclusion of pore size into models describing ceramic foam properties should be sought, since L has a higher degree of variability than ε for most cellular ceramic structures found in the literature. This ought to be a topic of a future study.

Acknowledgements

The authors gratefully acknowledge the financial support of the “Fundação para a Ciência e a Tecnologia” (FCT) under contract POCTI/CTM/35470/00. We would like also to acknowledge the technical assistance of C. Anjinho (at IST) and P. Coelho (at INETI). Special thanks are extended to D. Dias from Rauschert Portuguesa Ltd. and A. Moreira from Flexipol – Espumas Sintéticas S.A. for supplying the raw materials and the PU foams used in this study. One of us – S. Dias – thanks FCT for a grant.

References

- Colombo, P., Ceramic foams: fabrication, properties and application. In *Key Engineering Materials*, Vols 206–213. Trans Tech Publications, Switzerland, 2002, pp. 1913–1918.
- Brezny, R. and Green, D. J., The effect of cell size on the mechanical behaviour of cellular materials. *Acta Metall. Mater.*, 1990, **38**(12), 2517–2526.
- Colombo, P., Hellmann, J. R. and Shelleman, D. L., Mechanical properties of silicon oxycarbide ceramic foams. *J. Am. Ceram. Soc.*, 2001, **84**(10), 2245–2251.
- Brezny, R. and Green, D. J., Fracture behavior of open-cell ceramics. *J. Am. Ceram. Soc.*, 1989, **72**(7), 1145–1152.
- Mukhopadhyay, S. M., Mahadev, N., Joshi, P., Roy, A. K., Kearns, K. M. and Anderson, D. P., Structural investigation of graphitic foam. *J. Appl. Phys.*, 2002, **91**(5), 3415–3420.
- Costa Oliveira, F. A., Franco, J., Cruz Fernandes, J. and Dias, D., Newly developed cordierite-zircon composites. *Br. Ceram. Trans.*, 2002, **101**(1), 14–21.
- Costa Oliveira, F. A., Dias, S., Mascarenhas, J., Ferreira, J. M. F., Olhero, S. and Dias, D., Fabrication of cellular cordierite foams. In *Materials Science Forum II*, Vols 455–456, ed. R. Martins et al. Trans Tech Publications, Switzerland, 2004, pp. 177–181.
- Matos, M. J., Vaz, M. F., Cruz Fernandes, J. and Costa Oliveira, F. A., Structure of cellular cordierite foams. In *Materials Science Forum II*, Vols 455–456, ed. R. Martins et al. Trans Tech Publications, Switzerland, 2004, pp. 163–167.
- <http://www.mediacy.com>.
- R. de Hoff, F. N. Rhines, *Microscopie Quantitative*. Ed. Massun et Cie. Paris, France, 1972.
- Costa Oliveira, F. A., Dias, S., Vaz, M. F. and Cruz Fernandes, J., Crushing behaviour of cellular cordierite foams. In *Materials Science Forum II*, Vols 455–456, ed. R. Martins et al. Trans Tech Publications, Switzerland, 2004, pp. 172–176.
- Ashby, M. F., The mechanical properties of cellular solids. *Metall. Trans. A*, 1983, **14A**, 1755–1769.
- Gibson, L. G. and Ashby, M. F., *Cellular Solids Structure & Properties*. Cambridge University Press, Cambridge, UK, 1997.
- Maiti, S. K., Gibson, L. J. and Ashby, M. F., Deformation and energy absorption diagrams for cellular solids. *Acta Metall.*, 1984, **32**(11), 1963–1975.
- Brezny, R. and Green, D. J., Uniaxial strength behavior of brittle cellular materials. *J. Am. Ceram. Soc.*, 1993, **76**(9), 2185–2192.
- Brezny, R. and Green, D. J., Mechanical behavior of cellular ceramics. In *Materials Science and Technology—A Comprehensive Treatment. Structure and Properties of Ceramics*, Vol 11, ed. R. W. Cahn, P. Haasen and E. J. Kramer. VCH, Weinheim, Germany, 1994, pp. 463–516.
- Dam, C. Q., Brezny, R. and Green, D. J., Compressive behavior and deformation-mode map of an open cell alumina. *J. Mater. Res.*, 1990, **5**(1), 163–171.
- Hagiwara, H. and Green, D. J., Elastic behavior of open-cell alumina. *J. Am. Ceram. Soc.*, 1987, **70**(11), 811–815.
- Brezny, R., Green, D. J. and Dam, C. Q., Evaluation of strut strength in open-cell ceramics. *J. Am. Ceram. Soc.*, 1989, **72**(6), 885–889.